**10.6** LIDAR OBSERVATIONS OF ENTRAINMENT ZONE STRUCTURE AT THE TOP OF THE STABLE MARINE ATMOSPHERIC BOUNDARY LAYER

Ian M. Brooks*
Scripps Institution of Oceanography, La Jolla, California

## 1. INTRODUCTION

Entrainment is an important factor in the development of the boundary-layer (BL) and is a key process controlling the distribution and structure of boundary-layer clouds (Nicholls and Turton 1986). Most observational studies of entrainment zone structure have been undertaken under convective conditions, with the ultimate aim of relating the entrainment rate to the surface buoyancy flux and inversion properties. Few studies have examined stable conditions where wind shear is the sole driving force for entrainment. Price (1999) observed the breakup of stratocumulus under the influence of shear-driven entrainment but did not study the entrainment process in detail. Kiemle et al. (1998) compared the variability of local entrainment zone (EZ) depths of a stable boundary layer with those of several convective cases; they found the stable case to have a much narrower, more symmetric distribution.

Here we present some preliminary results of a study of entrainment zone structure for stable marine boundary layers off the coast of northern California. This abstract focuses on the cloud-topped case.

## 2. MEASUREMENTS AND PROCESSING

The measurements were made during the Coastal Waves 96 field program (Rogers et al. 1998) in June 1996, using the National Center for Atmospheric Research (NCAR) Scanning Aerosol Backscatter Lidar (SABL) flown on the NCAR C-130 Hercules. SABL operates at wavelengths of 532 and 1064 nm; the 1064 nm range corrected data is used for this study. All measurements were obtained while flying several hundred meters above cloud top. The vertical resolution of the lidar is 3.75 m; the horizontal resolution is approximately 5 m at a nominal airspeed of 100 m $s^{-1}$.

Cloud top is determined from the backscatter profiles by means of a wavelet covariance approach following that described by Davis et al. (2001); Brooks (2002) describes some of the problems and limitations encountered when applying this approach to non-ideal data. Figure 1 shows two typical backscatter profiles. Figure 2 shows the associated profiles of the wavelet covariance $W_f$ for several values of the wavelet dilation – positive/negative peaks in $W_f$ correspond to steps down/up in the backscatter signal, with a coherent scale equal to the wavelet dilation. Cloud produces a strong backscatter signal, often saturating the detector – the smooth gradient across the flattened peak of the profiles is due to the range correction being applied to the constant saturated signal. In spite of the strong signal from cloud top, a number of complications arise when attempting to define a completely automatic detection algorithm:

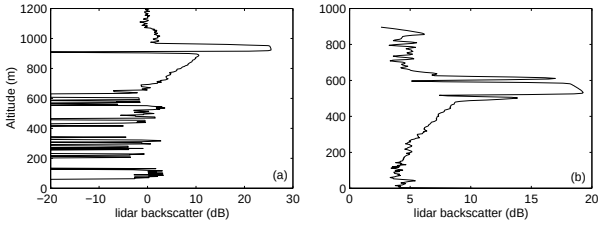


**Figure 1**. Typical profiles of lidar backscatter for a cloud-topped boundary layer.

- The signal is often completely attenuated below cloud, so that only instrument noise remains – after range correction this can have a substantial amplitude, and for small wavelet dilations may produce the strongest peaks in $W_f$.
- For a wavelet dilation greater than the thickness of the backscatter saturation peak b($W_{f\max}$) tends to occur when the lower edge of the wavelet aligns with the bottom of the saturation peak, and thus overestimate cloud top.
- Structure in thin cloud near its top can produce multiple peaks in the backscatter, as in figure 1(b); this can then produce multiple closely-spaced peaks in $W_f$.

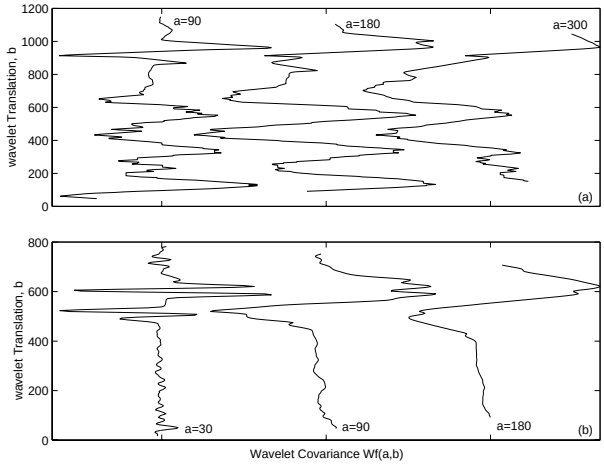


**Figure 2**. Profiles of the wavelet covariance $W_f$ for the two backscatter profiles shown in figure 1.

* *Corresponding Author address*: Ian M. Brooks, Integrative Oceanography Division, SIO-UCSD, 9500 Gilman Drive, La Jolla, CA. 92093-0209; email ibrooks@ucsd.edu

- When the lidar comes off its saturation peak, the amplifier may overshoot producing a negative spike, as in figure 1(a). The lower edge of this spike can produce the largest value of $W_f$ for small wavelet dilations. Note that the thickness of the saturated part of the backscatter signal is not related to cloud depth, but depends upon the degree to which the detector is overloaded.

These factors mean that, regardless of the dilation chosen, it is not possible to use the maximum in $W_f$ as representative of cloud top. In order to overcome these problems the following approach is adopted. A wavelet dilation of 90 m is used to generate a $W_f$ profile for each backscatter profile. Each individual peak for which $W_f > 0.7 W_{f\max}$ is identified, and the uppermost of these is selected as cloud top. Inspection of the resulting cloud-top series revealed a small number (~0.5%) of cloud top values that departed significantly from their near-neighbors. A 3-point median filter is applied to correct the outliers – defined as any point differing by more than 3 range gates from its median filtered value).

## 3. RESULTS

A total of 12 sections of flight legs over cloud are analyzed, drawn from flights on the 12th and 21st of June. Some flight legs have been split into multiple sections where the mean properties change visibly along the leg. Figure 3 shows histograms of cloud top heights for each section. Not all the variation in cloud top is due to turbulence structures associated with entrainment mixing; mesoscale variability in boundary layer depth and gravity waves also contribute. In order to isolate the smaller-scale variability associated with entrainment we high-pass filter the cloud top data

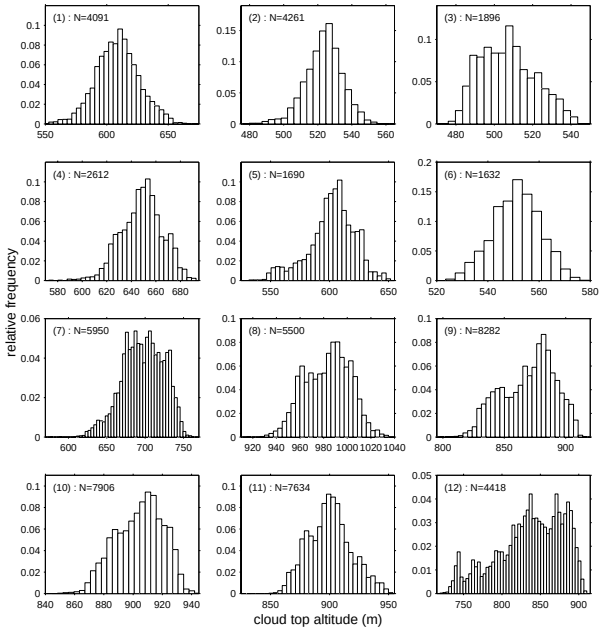


**Figure 3**. Histograms of cloud top height. The number of samples in each section is indicated on the figure.

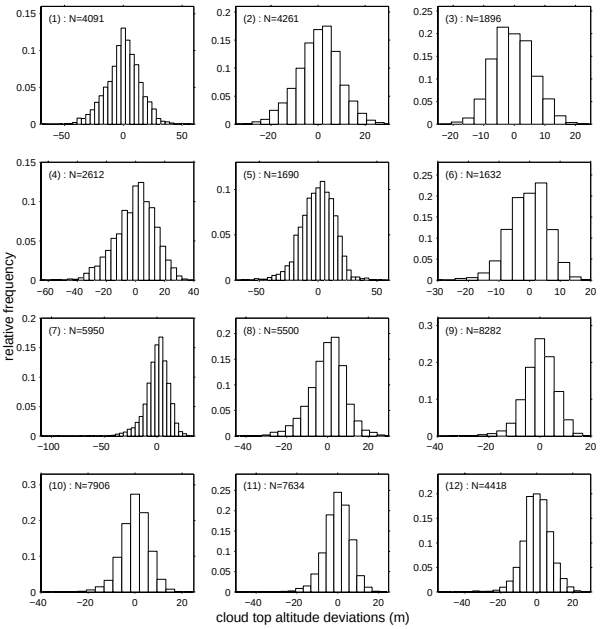


**Figure 4**. Histograms of high-pass filtered cloud top heights.

series; imposing a pass-band limiting wavelength of 2 km and a cut-off wavelength of 3.5 km. These values were chosen after careful inspection of the cloud-tip series and their power spectra. Figure 4 shows the resulting histograms of filtered cloud top height; these are now representative of the variation in cloud top height that defines a mean entrainment zone depth. The EZ is commonly defined as the region for which the cumulative frequency of boundary layer top lies between two limiting values – 5% and 95% are common choices but the exact values chosen have varied between studies (Deardorff et al. 1980, Wilde 1980, Melfi et al. 1985). We adopt values of 5% and 95%. The EZ depths are listed in table 1 along with other statistical properties of the filtered cloud top heights. The EZ depth and cloud-top height distributions are much narrower than those typically observed for convective conditions over land, where it may reach a depth of several hundred meters (eg Davis et al. 1997). Boer et al (1988) presented observations of cloud-top heights for a

**Table 1**. Statistical properties of filtered cloud top heights

| | $z_i$ | EZ Depth | Std. Dev. | Skew | Kurtosis |
|---|---|---|---|---|---|
| June 12 | | | | | |
| (1) | 608 | 48.0 | 14.2 | -0.228 | 0.48 |
| (2) | 523 | 30.9 | 9.0 | -0.204 | 0.21 |
| (3) | 507 | 22.3 | 6.5 | 0.157 | -0.17 |
| (4) | 649 | 45.0 | 13.6 | -0.469 | 0.31 |
| (5) | 602 | 45.3 | 14.1 | -0.344 | 0.81 |
| (6) | 551 | 20.9 | 6.4 | -0.393 | 0.40 |
| (7) | 697 | 35.6 | 11.0 | -1.117 | 4.46 |
| June 21 | | | | | |
| (8) | 983 | 29.1 | 8.8 | -0.462 | 0.95 |
| (9) | 870 | 20.2 | 6.2 | -0.557 | 1.25 |
| (10) | 903 | 19.3 | 5.9 | -0.462 | 1.08 |
| (11) | 899 | 21.0 | 6.3 | -0.515 | 1.24 |
| (12) | 837 | 25.0 | 7.7 | -0.497 | 2.01 |

marine stratocumulus deck under convective conditions. They found standard deviations of about 30-40 m, several times the values observed here. The skewness values, however, are very similar for both studies, indicating that the shape of the cloud tops is similar, although they differ in scale. The predominantly negative skewness indicates that there are more points above the mean value than below – the clouds tend to have flattened tops with narrower regions of clear air penetrating down into the BL, as might be expected for cloud capped by a strong inversion.

The depth of the entrainment zone has been observed to be correlated with that of the boundary layer for convective cases, so that the inversion height, $z_i$, is often used to scale the EZ depth (Davis et al. 1997). Figure 5 shows EZ depth plotted against $z_i$ for the present study – it is clear that there is no correlation between the two under stable conditions; thus an alternative scaling length must be sought for the EZ over stable boundary layers.

Figure 6 shows power spectra of the unfiltered cloud top heights. There is a clear -5/3 slope at high frequencies for all cases, but the low frequency behavior differs between the two days. On June 12 (runs 1-7) there is a distinct change in gradient at frequency between 0.05 and 0.2 Hz (wavelengths of 2 km and 0.5 km). On June 21 (runs 8-12) the upper limit of the -5/3 slope is less well defined, and runs (9) and (12) maintain the same gradient across all scales; there is no consistent behavior at larger scales. Boers et al. (1988) also found a -5/3 slope at small scales; it implies the presence of an inertial subrange for cloud top heights and hence a direct correlation between small-scale variations in cloud-top height and in-cloud turbulence. They noted that the scale at which the slope of their spectrum changed (~900m) was the same as the BL depth. No such correlation is observed here. Boers et al. found a consistent spectral peak in their cloud-top spectra, at a wavelength of about 4.5 km, with the spectral energy decreasing at larger scales. No significant decrease in spectral energy is observed on any of the runs examined here, though some of the June 12 spectra show local minima at scales of between 2 and 4 km. All of these observations were made close to the coast, in regions of significant spatial variability in both mean and turbulent quantities. It is likely that mesoscale variability inherent in the near-coast environment is responsible for the high spectral energy observed at large scales in the present data set.

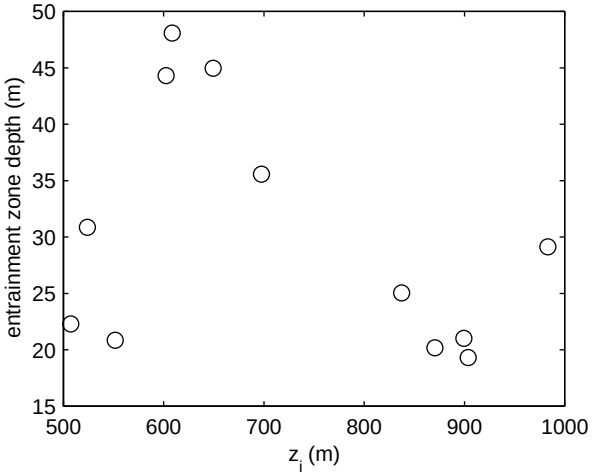


**Figure 5**. Entrainment zone depth plotted against boundary layer depth.

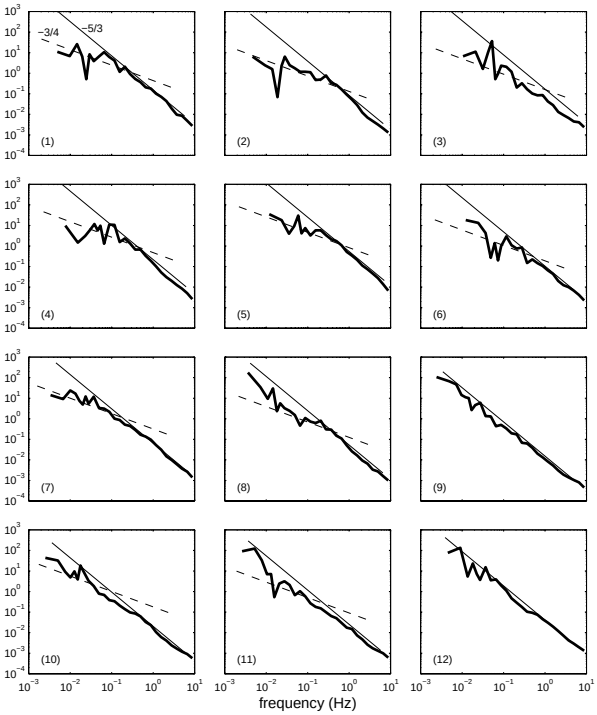


**Figure 6**. Power spectra of the unfiltered cloud top altitudes. Gradients of -5/3 and -3/4 are marked as thin solid and dashed lines respectively. The frequency scale corresponds to wavelengths of 100 km down to 10 m.

## 4. SUMMARY

We have presented preliminary results from a study of cloud-top and entrainment zone structure for a stable marine atmospheric boundary layer, based on airborne lidar measurements. The high spatial resolution of measurements available from the SABL lidar has enabled the small-scale structures prevalent under stable conditions to be mapped in detail. The variability in cloud top height is much smaller than that observed for marine stratocumulus clouds under convective conditions, and the entrainment zone similarly much narrower. The similarity in the skewness of the cloud-top statistics for stable and convective cases, nevertheless implies that the while the scales differ, the shape of the cloud tops is similar. Under convective conditions the entrainment zone depth has been found to scale with the boundary layer depth. Here we find no correlation between the two – as we might expect for stable conditions, where turbulence in throughout the bulk of

the boundary layer does not 'feel' the influence of the surface. This means that alternative scaling lengths must be sought for the entrainment zone depth under stable stratification. An evaluation of the relationship between the entrainment zone and inversion layer properties such as wind shear and stratification is in progress.

Power spectra of the unfiltered cloud top heights show a -5/3 slope for smaller scales (<~500 m - 2 km) on all 12 data sections. At large scales the behavior differs between the two days. On June 12$^{th}$ there is a decrease in the gradient to ~3/4, while on June 21$^{st}$ there is no clear systematic behavior at large scales. The presence of a -5/3 slope implies the existence of an inertial subrange, and a direct correlation between in-cloud turbulence and the variability of cloud top. The high spectral energy at large scales is attributed to the mesoscale variability in boundary layer depth inherent in the near-coast flow.

***Acknowledgements***. This work was supported by the National Science Foundation: grant ATM-0100685, and the Office of Naval Research: grant N00014-01-1-0258.

**REFERENCES**

Boers, R. J. D. Spinhirne, and W. D. Hart, 1988: Lidar observations of the fine-scale variability of marine stratocumulus clouds. *J. Appl. Meteorol.*, **27**, 797-810.

Brooks, I. M., 2002: Finding Boundary Layer Top for the Stable Layer: Application of a Haar Wavelet Covariance Transform to Lidar Observation. *This Volume.*

Davis, K. J., D. H. Lenschow, S. P. Oncley, C. Kiemle, G. Ehret, and A. Giez, 1997: Role of entrainment in surface-atmosphere interactions over a boreal forest. *J. Geophys. Res.*, **102**, 29219-29230.

Davis, K. J., N. Gamage, C. R. Hagelberg, C. Kiemle, D. H. Lenschow, and P. P. Sullivan, 2000: An objective method for deriving atmospheric structure from airborne lidar observations. *J. Atmos. Oceanic. Technol.*, **17**, 1455-1468.

Deardorff, J. W., G. E. Willis, and B. H. Stockton, 1980: Laboratory studies of the entrainment zone of a convectively mixed layer. *J. Fluid. Mech.*, **100**, 41-64.

Kiemle, C., G. Ehret, and K. J. Davis, 1998: Airborne lidar studies of the entrainment zone. *Proceedings 19$^{th}$ International Conf. on Laser Radar*, Annapolis, 395-398.

Melfi, S. H., J. D. Sphinhirne, S. H. Chou, and S. P. Palm, 1985: Lidar observations of the vertically organized convection in the planetary boundary layer over the ocean. *J. climate Appl. Meteorol.*, **24**, 806-821.

Nicholls, S., and J. D. Turton, 1986: An observational study of the structure of stratiform cloud sheets: part 2. Entrainment. *Quart. J. Royal. Meteorol. Soc.*, **112**, 461-480.

Price, J. D., 1999: Observations of stratocumulus cloud break-up over land. *Quart. J. Royal. Meteorol. Soc.*, **125**, 441-468.

Rogers, D. P., C. Dorman, K. Edwards, I. Brooks, K. Melville, S. Burk, W. T. Thompson, T. Holt, L. Ström, M. Tjernström, B. Grisogono, J. Bane, W. Nuss, B. Morley, and A. Schanot, 1998: Highlights of Coastal Waves 1996. Bull. Amer. Meteorol. Soc., **79**, 1307-1326.

Wilde, N. P., R. B. Stull. and E. W. Eloranta, 1985: The LCL zone and cumulus onset. *J. Climate Appl. Meteorol.*, **24**, 640-657.